

# ELECTROKINETIC STABILISATION OF ENGINEERED SAND BACKFILL ADMIXED WITH RECYCLED TYRE WASTES

\*Chee-Ming Chan<sup>1</sup>, An-Shang Chang<sup>2</sup>, Salina Sani<sup>1</sup> and Siti Farhanah SM Johan<sup>3</sup>

<sup>1</sup>Research Centre for Soft Soils (RECESS), Universiti Tun Hussein Onn Malaysia, Malaysia;

<sup>2</sup>CAGA Consultants Pte. Ltd., Singapore; <sup>3</sup>Faculty of Engineering, Universiti Malaysia Sarawak, Malaysia

\*Corresponding Author, Received: 06 Dec. 2025, Revised: 29 Jan. 2026, Accepted: 30 Jan. 2026

**ABSTRACT:** Malaysia's abundant sand resources support construction, manufacturing and geotechnical works such as embankment backfills, but rising demand and intensive extraction have increased environmental pressures, especially in sensitive coastal zones. This study examines a sustainable approach to improving sand-based backfill materials through electrokinetic (EK) stabilisation combined with recycled crumb rubber and steel fibres from waste tyres. EK stabilisation enhances soil behaviour via electro-osmotic flow, ionic migration and mineral precipitation, improving shear strength, consolidation and permeability characteristics of the soil. Crumb rubber contributes ductility and energy absorption, while steel fibres increase tensile strength and load-bearing capacity. Mixtures containing 10–40% crumb rubber, 1–4% steel fibres, and 4% proprietary polymer-modified cementitious soil stabiliser (PMC) for enhanced structuration were evaluated to identify optimal shear strength and moisture-management performance. Results show that EK treatment promotes mineral-based aggregation and fabric restructuring, producing microstructural densification and cementation that markedly increase undrained shear strength ( $c_u$ ) even without significant moisture reduction. The EK-stabilised rubber–steel fibre system offers a promising solution for developing stronger and more resilient backfill materials for sustainable geotechnical applications.

*Keywords: Electrokinetic Stabilization; Sand; Rubber Wastes; Shear Strength; Ionic Migration*

## 1. INTRODUCTION

Malaysia's sand remains a critical natural resource, heavily relied upon by industries such as construction, glass manufacturing and electronics. Given the continued abundance of reserves, especially in East Malaysia's coastal regions, sand remains integral to the nation's infrastructural and industrial growth [1–2]. Its high silica content makes it particularly suitable for producing concrete, bricks and premium-grade glass products. Beyond industrial applications, sand is also widely used as an engineered backfill material in geotechnical and coastal projects, such as land reclamation, embankment fill, erosion control and stabilising shorelines. These uses emphasise sand's role not only in construction but also in environmental and infrastructure resilience.

However, accelerated urbanisation and the expanding construction sector have intensified sand mining activities across the nation. This surge in extraction has led to significant environmental degradation, including coastal erosion, habitat destruction and water pollution, particularly in sensitive coastal zones [3]. Therefore, comprehensive regulatory frameworks and coastal management strategies are now being considered to ensure sustainable utilisation of sand resources in such applications.

In response, research has shifted toward alternative materials and stabilisation techniques that

enhance the performance of existing sand and backfill resources while reducing ecological harm. Among these, electrokinetic (EK) stabilisation has emerged as a promising method for improving the geotechnical and mechanical properties of soils and backfilled materials. EK stabilisation employs electrical fields to induce electro-osmotic flow and ionic migration, resulting in enhanced undrained shear strength ( $c_u$ ), permeability and consolidation [4–5].

Simultaneously, the incorporation of recycled waste materials such as crumb rubber and steel fibres from used tyres supports sustainable waste management while enhancing soil geotechnical performance [6–7]. Under EK treatment, these additives can modify soil behaviour through improvements in strength, ductility, durability and ion transport driven by the applied electric field, thereby reinforcing the effectiveness of EK stabilisation [8–9]. Crumb rubber improves energy absorption and crack resistance, whereas steel fibres enhance tensile strength and load-bearing capacity; however, the combined effects of rubber, steel fibre and chemical binders under EK treatment, particularly in relation to electrode degradation and  $Fe^{3+}$  mobilization, remain largely unexplored [10–11]. In addition, the cost implications of EK-assisted stabilisation, including potential material savings and improved treatment efficiency, have received limited attention in the existing literature.

The significance of this study lies in its original integration of recycled crumb rubber, steel fibres and

chemical binders within EK treatment, addressing key gaps in soil mechanical performance, electrode durability and microstructural strengthening. The findings identify effective material compositions that enhance strength and moisture regulation in EK-treated soils, providing practical guidance for engineering applications. It represents a novel and sustainable stabilization framework for improving the performance of sand-based backfill materials in geotechnical practice.

## 2. RESEARCH SIGNIFICANCE

This study presents a novel integration of electrokinetic (EK) stabilization with recycled tyre-derived crumb rubber, steel fibres and a polymer-modified cementitious binder for engineered sand backfill applications. Unlike previous studies that investigated these materials separately, this research evaluates their combined effects on shear strength, moisture migration, electrode degradation and  $Fe^{3+}$  mobilization under EK treatment. The findings establish an original and sustainable stabilization framework for enhancing the performance and durability of sand-based backfill materials.

## 3. MATERIALS AND METHODS

### 3.1 Test Materials

The materials used in this study included river sand, clay, recycled rubber powder, recycled steel fibres, a proprietary polymer-modified cementitious soil stabiliser (PMC; primary contents of cement and lime ~85%) and deionised water.

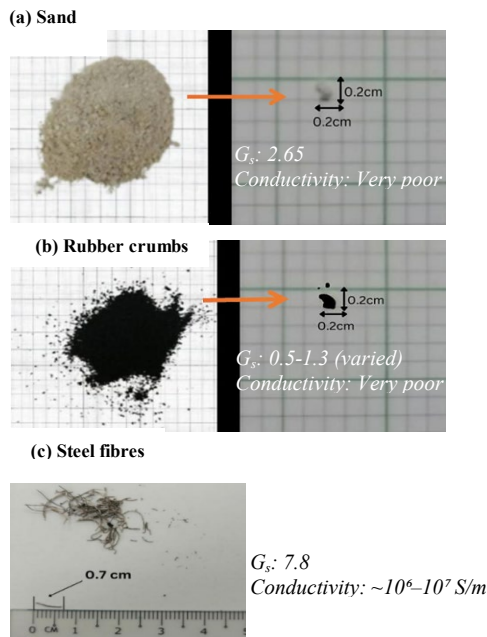


Fig. 1 Materials used in the study

The sand was sourced from a river and subsequently sieved to ensure that all particles used in the mixtures were smaller than 2 mm. Recycled rubber was incorporated as particles of nominal size less than 2 mm too, while recycled steel fibres with lengths under 1 cm were used as the fibrous additive (Figure 1). These materials were combined with sand to create 4 general sample types. To determine the optimum mixing ratio of recycled rubber and steel fibres, a total of 9 EK stabilisation model designs were prepared.

### 3.2 Electrokinetic (EK) Test Chamber

Figure 2 illustrates the electrical setup, wire arrangement and overall system dimensions. Stainless steel electrodes measuring 10 mm in diameter and 120 mm in length were used in this study. Stainless steel was selected due to its high electrical conductivity, corrosion resistance in oxygenated water and cost-effectiveness when applied over large treatment areas. The electrodes, functioning as the anode and cathode, were positioned 50 mm apart to ensure effective electric field distribution during the EK treatment. This size is consistent with prior studies on compact specimens typically 30–60 mm, allowing measurable changes in soil properties without introducing artefacts such as localized heating or rapid drying. Copper wire was used to establish reliable electrical connections between the electrodes and the power supply. A 5 V, 4 A AC–DC converter, connected to the copper wires and then to the electrodes, provided the electrical input for the electrokinetic (EK) dewatering process. Note that the electrode configuration and power input were chosen to ensure EK efficiency within practical limits of scale-up, maintenance and energy use.

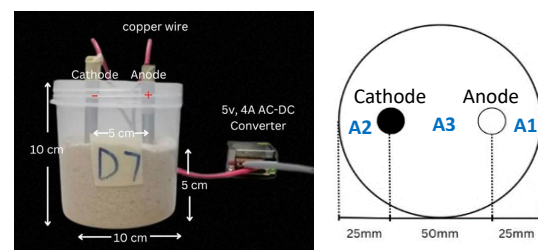


Fig. 2 The electrokinetic test chamber

### 3.3 Sample and Test Setup

The sand was admixed with deionised water until a fully saturated condition was achieved. The saturated sand was then placed in the cylindrical test chamber in 5 loose layers, where each layer was gently tapped to release the entrapped air. The final compacted uniform sand layer measured 50 mm in height. The prepared sand–water mixture was next sealed to rest for 24 hours to allow uniform moisture

distribution. Following 24-hour equilibration, the stainless steel electrodes were inserted to the bottom of the specimen with a fixed spacing of 50 mm. The same procedure was repeated for all sample variations: (i) base sample 40% clay + 60% sand; (ii) clay-sand mixture with recycled rubber; (iii) clay-sand mixture with recycled rubber and steel fibre; and (iv) clay sand mixture with recycled rubber, steel fibre and PMC.

### 3.4 Vane shear test

The test was conducted per BS 1377 Pt. 7 [12] to determine undrained shear strength,  $c_u$ . A 4-bladed vane, 25 mm wide, 60 mm high and 16 mm across each blade, was carefully inserted into the specimen and rotated at a constant rate of 0.1–0.2°/s until failure. The torque (T) required to initiate soil shear was recorded, and  $c_u$  was determined by division of T with the spring constant, K.

## 4. RESULTS: ANALYSIS AND DISCUSSIONS

Following the experimental procedures outlined in the previous section, this part analyzes and discusses the results of the electrokinetic stabilization tests. A 7-day curing period was adopted in line with standard field stabilization practice to assess early-stage performance.

### 4.1 Unsterilized Behaviour without Electrokinetic Treatment

Essentially samples of sand and clay-sand mixtures cured for 1 day, 4 days and 7 days were first examined without undergoing electrokinetic (EK) treatment. This procedure was carried out to evaluate whether the soils could achieve adequate  $c_u$  naturally, in the absence of EK stabilisation. The same procedure was then carried out for samples admixed with rubber crumbs and steel fibres as reinforcement elements for the soil mixture. Baseline mechanical properties were evaluated using vane shear tests and moisture content measurements prior to any EK stabilisation, providing an initial understanding of the engineered sand backfill's inherent strength and behaviour.

#### 4.1.1 Sand

Table 1(a) reports the undrained shear strength ( $c_u$ ) measured at 5 positions within each sample, i.e., top, middle, anode, cathode and bottom, after each curing interval. In the control specimens (100% sand without EK treatment), vane shear tests revealed initially modest cohesion due to capillary and adsorbed water effects: On Day 1,  $c_u$  was relatively uniform (1.8-2.0  $\text{Nm}^{-2}$ ), indicating that moisture-induced apparent cohesion dominated. By Day 4,  $c_u$  dropped sharply to around 0.6  $\text{Nm}^{-2}$  at all positions,

suggesting that as evaporation proceeded, the capillary bridges collapsed or lost tension, thereby reducing interparticle bonds. The strength remained at this lower level through Day 7, indicating that the sand reached an equilibrium state where further moisture loss did not lead to more significant cohesion loss.

These results highlight the intrinsic limitation of relying on water-induced cohesion in pure sand: while initial moisture can sustain a low level of apparent  $c_u$ , the loss of water through drying quickly degrades shear strength. This observation is consistent with studies by Ahmad & Uchimura [13] showing that increasing moisture can first increase cohesion via capillary stress but then diminish it as water films lubricate particles and reduce interparticle bonding.

#### 4.1.2 Clay-sand

Table 1(b) records the evolution of  $c_u$  in clay-sand specimens over a 1-week curing period under natural conditions, i.e. no EK treatment. On Day 1,  $c_u$  was uniformly low ( $\approx 0.2 \text{ Nm}^{-2}$ ), reflecting the initially loose, unconsolidated state of the mixture with minimal interparticle bonding. By Day 4,  $c_u$  had increased substantially (2.0-3.6  $\text{Nm}^{-2}$ ), indicating the onset of natural consolidation: Water redistribution within the pore space, particle rearrangement and capillary forces begin to draw particles closer, enhancing initial cohesion and mechanical interaction. By Day 7,  $c_u$  continued to rise (3.2-5.2  $\text{Nm}^{-2}$ ) and showed more spatial variability, suggesting that further consolidation and progressive interparticle bonding, possibly via adsorbed water films and clay bridging, were strengthening the mixture unevenly across locations.

Table 1.  $c_u$  measured at various test points for the clay-sand (CS) soil samples

Test Points	Top	Middle	Cathode	Anode	Bottom
Days	Undrained shear strength, $c_u$ ( $\text{N/m}^2$ )				
(a) Sand					
Day 1	2.0	1.8	2.0	2.0	1.8
Day 4	0.6	0.6	0.6	0.6	0.6
Day 7	0.6	0.4	0.6	0.6	0.6
(b) Sand-Clay					
Day 1	0.2	0.2	0.2	0.2	0.2
Day 4	3.6	2.4	2.0	2.8	3.0
Day 7	4.2	3.2	5.2	4.4	3.8

These trends illustrate that even without electrochemical intervention, clay-sand mixtures can develop significant strength gain over time, driven by moisture migration, particle reorientation and

consolidation mechanisms. This behaviour aligns with findings by Karakan & Demir [14] showing how clay content promotes consolidation-driven strength gain: As fines fill the voids, interparticle contacts improve and the mixture’s cohesion increases.

#### 4.1.3 Clay-sand rubber

The variation in  $c_u$  over time for clay-sand samples containing different rubber dosages are presented in Table 2. A general trend of increasing  $c_u$  over the curing period was observed for most compositions.

Table 2.  $c_u$  of sand-clay admixed with rubber crumbs (R)

Test points	R-10%	R-20%	R-30%	R-40%
Days	Undrained shear strength, $c_u$ (n/m <sup>2</sup> )			
Day 1	1.6	1.1	0.6	1.9
Day 4	3.2	3.7	1.8	2.9
Day 7	4.7	5.0	4.5	4.2

A general trend of increasing  $c_u$  over the curing period was observed for most compositions. The 20% soil-rubber mixture achieved the highest  $c_u$  of 5.0 Nm<sup>-2</sup> on Day 7, whereas the 40% soil-rubber mixture exhibited the lowest value of 4.2 Nm<sup>-2</sup> at the same time. These results indicate that the inclusion of rubber can enhance  $c_u$  up to an optimal content, beyond which further addition may reduce performance. This finding aligns with Akbarimehr et al. [15] who reported that adding rubber improves  $c_u$  by 10-25% at moderate levels, but excessive rubber portions can diminish the soil’s mechanical properties. Thus, a 20% rubber content appears optimal for strengthening clay-sand mixtures under natural curing conditions.

Also, reviewing Table 3, it is apparent that increasing the proportion of rubber in clay-sand mixtures leads to a consistent reduction in moisture content over time. For example, the CS-90% R-10% mixture exhibited a moisture content of 24.7% on Day 1, which decreased to 17.2% on Day 4 and further dropped to 5.6% on Day 7. Similar trends were observed for the CS-80% R-20%, CS-70% R-30% and CS-60% R-40% mixtures, all showing progressive drying over the observation period. This behaviour aligns with recent findings by the utilization of recycled rubber crumbs as part of the additives to enhance clayey soil performance [16], which reported that increasing crumbled-rubber content reduces the soil’s capacity to retain water, thereby lowering its liquid and plastic limits and optimum moisture content. These results indicate that higher rubber content accelerates moisture reduction in clay-sand mixtures, underscoring the role of rubber in modifying drying behaviour and moisture

retention characteristics of stabilised soils.

Table 3. \*Moisture content of sand-clay admixed with rubber crumbs (R)

Sample	Cs90-r10	Cs80-r20	Cs70-r30	Cs60-r40
Days	Moisture content (%)			
Day 1	24.7	25.1	27.0	27.5
Day 4	17.2	16.4	19.5	19.5
Day 7	5.6	5.6	19.5	5.0

\*Samples were oven-dried at 105°C- 24 hours; BS1377 Pt. 2 [12].

#### 4.1.4 Clay-sand rubber + steel fibres

Table 4 depicts the variation in  $c_u$  over time for clay-sand-rubber samples reinforced with different steel fibre contents. In general,  $c_u$  exhibited fluctuations during the curing period. The 3% steel fibre composition achieved a maximum of 5.80 Nm<sup>-2</sup> on Day 4 but declined to 5.00 Nm<sup>-2</sup> by Day 7. In contrast, the 4% steel fibre composition showed a steady increase from Day 1 to Day 7, ultimately reaching 5.80 Nm<sup>-2</sup>, thus demonstrating both strength and stability. Overall, the 4% soil-rubber and steel fibre composition provided the strongest and most stable enhancement of  $c_u$ . These findings align with recent research indicating that the inclusion of steel fibres in soil-cement matrices or fibre-reinforced soil blocks significantly improves  $c_u$  and ductility [9&17]. Therefore, similar improved performance can be expected of the soil-based innovation examined presently.

Table 4.  $c_u$  of sand-clay-rubber admixed with steel fibres (SF)

Sample	Sf 1%	Sf 2%	Sf 3%	Sf 4%
Days	Undrained shear strength, $c_u$ (n/m <sup>2</sup> )			
Day 1	1.8	1.3	1.4	1.6
Day 4	4.2	5.4	5.8	4.7
Day 7	5.3	4.9	5.0	5.8

Table 5 illustrates the variation in moisture content over time for clay-sand-rubber mixtures containing different proportions of steel fibre. In general, all compositions showed a continuous decline in moisture content during the curing period. The mixture with 4% steel fibre exhibited the largest reduction, reaching 11.3% moisture content by Day 7. In contrast, the 1%, 2% and 3% steel fibre mixtures converged to moisture contents around 12.0% on Day 7. These results suggest that increasing steel fibre content enhances the efficiency of the electrokinetic (EK) treatment: A higher concentration of conductive steel fibres promotes greater current flow through the soil matrix, thereby accelerating ion migration and electrochemical reactions, which in turn facilitate faster moisture removal. This is supported by Zafar et al. [17] in their review of synthetic fibre soil

stabilisation, which highlights how fibres improve hydraulic performance and water loss in treated soils.

Table 5. Moisture content of sand-clay-rubber admixed with steel fibres (SF)

Sample	Sf 1%	Sf 2%	Sf 3%	Sf 4%
Days	Moisture content (%)			
Day 1	22.0	22.0	23.1	22.0
Day 4	17.5	16.1	16.1	15.4
Day 7	12.7	12.9	12.3	11.3

**4.2 Stabilised Behaviour without Electrokinetic Treatment**

From the systematic evaluation discussed above, the optimal  $c_u$  and moisture content performance were achieved with a sand-clay mixture containing 20% rubber and 4% steel fibre. This specific blend, designated 80CS20R4SF, was further admixed with 4% of PMC. It was found to exhibit superior  $c_u$  during electrokinetic treatment, where monitoring over periods of 1, 4 and 7 days consistently demonstrated the effectiveness of this composition. With a fixed 4% PMC content, this balanced mixture not only enhanced  $c_u$  but also effectively regulated moisture content, as elaborated below

Figure 3 illustrates the variations in  $c_u$  over time for mixtures containing 4% PMC. Overall,  $c_u$  exhibited a gradual decline during the testing period. On Day 1,  $c_u$  ranged from 8.0  $Nm^{-2}$  to 11.6  $Nm^{-2}$ , reflecting the immediate reinforcement effect of the PMC. By day 7,  $c_u$  decreased significantly to a range of 2.0  $Nm^{-2}$  to 5.2  $Nm^{-2}$ , indicating a loss of binding efficiency over time. The results demonstrate that the 4% PMC mixture is most effective in achieving high initial  $c_u$ . These findings align with recent research that demonstrates how polymeric agents can significantly improve soil strength and water stability, such as by Li et al. [18] who strength increment up to 25% with polymeric stabilizer treatment of construction-waste soil mixture.

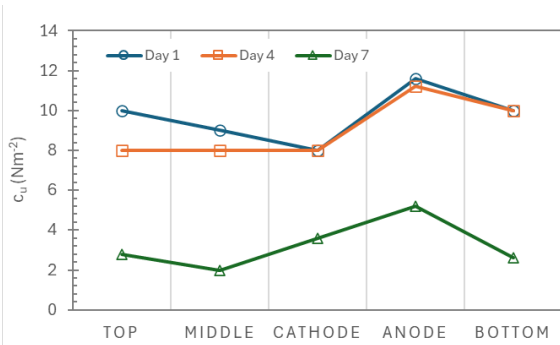


Fig. 3 Evolution of  $c_u$  for 80CS20R4SF+4%PMC over 1 week

The observed behaviour can be explained by the

chemical action of PMC. Upon hydration, PMC reacts with water to form calcium silicate hydrate (C–S–H) crystals, which act as a binding matrix, cementing the soil particles together and enhancing initial mechanical strength. During the EK test, water migration and reduction in moisture content limit the continued formation of C–S–H crystals, leading to a progressive decrease in  $c_u$  over time [19-20]. Additionally, the presence of rubber and steel fibre in the mixture provides mechanical interlocking and energy dissipation, which contributes to shear resistance initially but cannot fully compensate for the reduction in binder formation as the system dries. The results emphasize the necessity of integrating chemical and mechanical reinforcement approaches to achieve optimal  $c_u$ , both in the short term and over extended periods [21].

The variations in moisture content observed across the tested samples over time are presented in Figure 4. Sample A1 exhibited a substantial decrease in moisture content, declining from 22.2% on Day 1 to 9.1% on Day 7. Similarly, Sample A2 showed a consistent reduction, dropping from 22.2% on Day 1 to 10.0% on Day 7. In contrast, Sample A3 demonstrated a slight increase, reaching 10.7% on Day 7 from an initial 23.0% on Day 1, indicating a relatively slower water loss. These observations suggest that the samples exhibit distinct moisture retention behaviours, which can be attributed to differences in composition and microstructural characteristics.

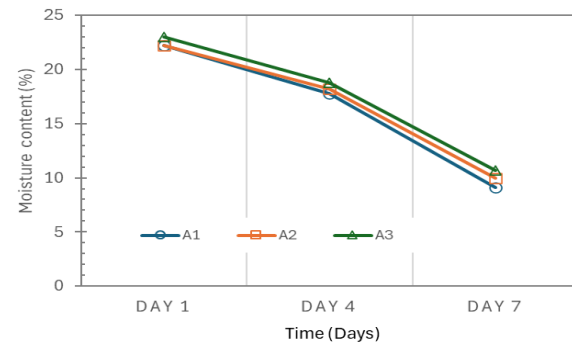


Fig. 4 Variation of moisture content for 80CS20R4SF+4%PMC over 1 week

The pronounced drying in Samples A1 and A2 may result from more efficient water migration during the electrokinetic (EK) process, enhanced by the conductive pathways provided by the mixture components, leading to rapid moisture removal. Conversely, Sample A3's slower reduction implies a higher inherent water retention capacity, potentially due to denser particle packing, greater polymer-modified chemical (PMC) content interaction with water, or the presence of additives that impede moisture migration. Understanding these variations is crucial for tailoring soil stabilisation strategies, as differential moisture behaviour directly impacts both

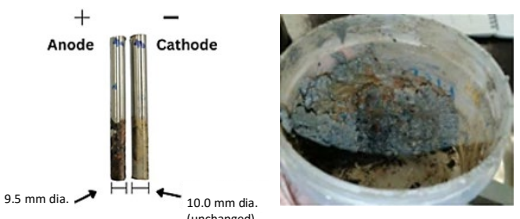
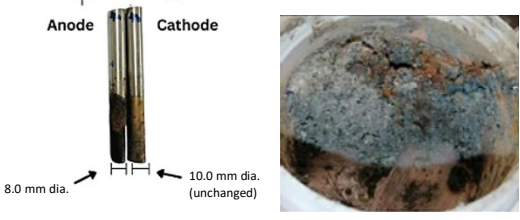
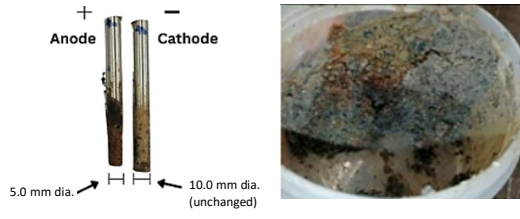
mechanical strength development and long-term durability of treated soils.

### 4.3 Stabilised Behaviour with Electrokinetic Treatment

#### 4.3.1 Electrode depletion

Table 6 summarizes the systematic variation of electrode sizes at intervals of 1, 4 and 7 days during the EK tests, implemented to assess the soil's evolving response to the applied electric field. Photographs in Table 6 illustrate the electrode conditions throughout the experimental period. A progressive reduction in the mass of the stainless-steel anode was observed from Day 1 to Day 7, while the cathode mass remained effectively constant, indicating a relatively inert cathodic environment and a stable electrochemical state during treatment.

Table 6. Changes in electrodes and Fe<sup>3+</sup> distribution

Electrodes condition	Fe <sup>3+</sup> distribution
 <p style="text-align: center;"><b>Day 1</b></p>	
 <p style="text-align: center;"><b>Day 4</b></p>	
 <p style="text-align: center;"><b>Day 7</b></p>	

The progressive reduction in the anode's mass indicates ongoing electrochemical reactions or material loss at the electrode-soil interface, attributed to oxidation or dissolution processes driven by the applied current. Pitting corrosion may develop due to localized breakdown of passive films too, especially in chloride-bearing pore water, accelerating mass loss. Han et al. [20] reported that electrode movement and chemical injection can reduce anode corrosion,

though electrochemical reactions still cause some material loss. Anode degradation can also be limited using corrosion-resistant electrodes (e.g. graphite or MMO-coated titanium), pH control and intermittent or polarity-reversal operation. Corrosion products, mainly Fe<sup>3+</sup> ions, precipitate as stable ferric hydroxides and are generally environmentally benign under typical EK stabilisation conditions. These observations highlight the dynamic electrode-soil interactions during EK treatment, with progressive anode mass loss reflecting corrosion, ion migration and electrochemical processes. Consistent with Ashour et al. [22], formation of C-S-H and other cementitious phases shows that released ions enhance soil bonding even as the anode corrodes, emphasizing the importance of electrode design for efficient, reliable EK treatment.

#### 4.3.2 Fe<sup>3+</sup> mobilization

An intriguing observation from the study was that the region surrounding the anode, where Fe<sup>3+</sup> ions were released, consistently exhibited the highest  $c_u$ . Despite the significant role of Fe<sup>3+</sup> in enhancing soil strength, the spatial extent of this Fe<sup>3+</sup>-influenced zone did not expand markedly over a week (Table 6), suggesting that the  $c_u$  improvement is highly localized and not directly proportional to the overall ion distribution. These findings, consistent with reports by Purkis et al. [23] and Xie et al. [24], highlight how site-specific chemical reactions during electrokinetic treatment can exert substantial mechanical effects.

Table 6 shows that variations in soil composition, including rubber, steel fibre and PMC, had little effect on Fe<sup>3+</sup> distribution, indicating that its release and mobility are mainly governed by intrinsic soil-electrochemical interactions controlling localized reinforcement and ion migration. PMC releases Ca<sup>2+</sup> and OH<sup>-</sup> into the pore fluid, enhancing ionic transport and conductivity. Electrolysis-generated H<sup>+</sup> and OH<sup>-</sup> react with these ions to form cementitious products (C-S-H, ettringite), densifying the microstructure and increasing stiffness. These combined chemical and electrokinetic effects explain the observed  $c_u$  gains, demonstrating that PMC acts synergistically with EK processes to strengthen the soil.

### 4.4 Correlation of $c_u$ and EK Treatment

Figure 5 relates the  $c_u$  values (see Figure 3) to the corresponding average water contents from Figure 4. Although the water content fluctuated within a relatively narrow range, the  $c_u$  values varied by nearly 50% between the upper and lower bounds. This indicates that the EK process can substantially enhance soil strength without requiring significant changes in moisture content. Such behaviour is notably characteristic of EK-stabilised soils, where strength gain arises primarily from physicochemical transformations rather than simple dewatering.

In EK treatment, the applied electric field drives ionic migration, electroosmosis and electromigration, promoting the transport and redistribution of stabilizing ions (e.g.  $\text{Fe}^{3+}$ ,  $\text{Ca}^{2+}$ ) within the soil matrix. These ions facilitate the formation of cementitious compounds such as C–S–H and C–A–H, which bind soil particles and refine the microstructure. Additionally, electrochemical reactions at the electrodes generate localized pH gradients that further enhance precipitation and bonding [25-26]. Together, these processes form a more integrated and rigid soil skeleton, reduce particle mobility and improve interparticle friction, even when the overall water content remains largely unchanged.

Thus, the observed spread in  $c_u$  values reflects the strong chemical and microstructural effects induced by EK mechanisms, demonstrating that soil strengthening can be achieved through electrically driven mineral formation and particle arrangement rather than through water removal alone. This is of particular importance in strengthening loose sand where effective compaction is not be feasible on site.

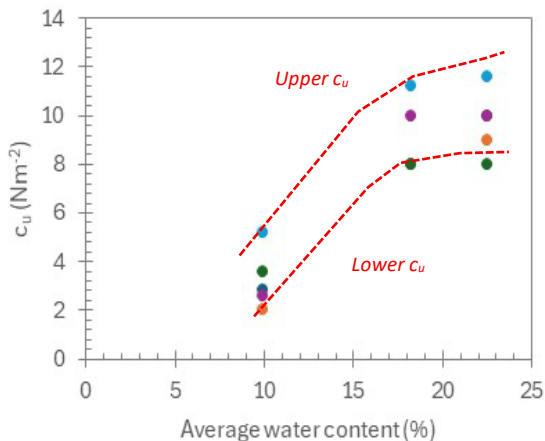


Fig. 5 Relationship between  $c_u$  and water content

## 5. CONCLUSIONS

The 80CS20R4SF sand-clay mixture with 4% PMC, 20% rubber and 4% steel fibres achieved the highest initial shear strength ( $c_u = 8.0\text{--}11.6 \text{ Nm}^{-2}$ ) while maintaining moisture between 22.2–23.0%. During EK treatment,  $c_u$  decreased to 2.0–5.2  $\text{Nm}^{-2}$  by Day 7 as C–S–H formation slowed, while moisture dropped to 9.1–10.7%, reflecting efficient water migration governed by composition and microstructure. Rubber and steel fibres enhanced mechanical interlocking, and PMC improved early strength, confirming that integrating chemical and mechanical reinforcement with EK treatment produces durable, high-performance and cost-efficient soil stabilisation.

The stainless-steel anode lost 50% mass over 7 days, while the cathode remained stable. Corrosion released  $\text{Fe}^{3+}$  ions, which precipitated as stable ferric hydroxides and contributed to C–S–H and other

cementitious phases, reinforcing soil bonding. EK increased  $c_u$  by nearly 50% across a narrow moisture range, demonstrating that strengthening arises primarily from electrically driven mineral formation and fabric restructuring rather than dewatering.

These findings highlight the synergistic interplay of chemical, mechanical, moisture and electrochemical processes. Recommendations include optimizing PMC and admixture proportions, using corrosion-resistant electrodes with pH or polarity control, as well as investigating  $\text{Fe}^{3+}$  migration and electrode–soil interactions to maximize localized and long-term EK stabilisation. The approach advances SDG 9.4 (resilient and sustainable infrastructure) and SDG 12.5 (waste reduction and resource efficiency) through reuse of tyre-derived materials and reduced virgin soil binder consumption in geotechnical solutions.

## 6. ACKNOWLEDGEMENT

Appreciation is due to Matching Grant Q625 by UTHM and technical support by Soil Instruments (M) S/B, RECESS and Geotechnology Lab at UTHM.

## 7. REFERENCES

- Mohammadian, E., Haron, A. S., Jafari, M., Liu, B., Azdarpour, A., and Ostadhassan, M., Integrated sand management: modeling of sand erosion in a mature oil field in Malaysia. *Geomechanics and Geophysics for Geo-Energy and Geo-Resources*, 10(1), 2024, pp. 4. <https://doi.org/10.1007/s40948-023-00723-z>
- Department of Mineral & Geoscience Malaysia. (2024). *Yearbook 2022-23: Silica Sand Production, Reserves and Uses in Malaysia*, pp. 1-84.
- Marine Coastal and Delta Sustainability for Malaysia. (2021). *Sand Mining*, pp. 1-10.
- Liu, P., Zhu, R., Zhao, F., and Zhao, Y., Enhancing dispersive soil: An experimental study on the efficacy of microbial, electrokinetics and chemical approaches. *Sustainability*, 16(23), 2024, pp. 10425. <https://doi.org/10.3390/su162310425>
- Pandey, B. K., Shukla, C., Sillanpää, M., and Shukla, S. K., A systematic review on application of electrokinetics in stabilisation and remediation of problematic soils. *Innovative Infrastructure Solutions*, 8(9), 2023, pp. 226. <https://doi.org/10.1007/s41062-023-01065-4>
- Hassan, M.R. and Rodrigue, D., Application of waste tire in construction: A road towards sustainability and circular economy. *Sustainability*, 16(9), 2024, pp. 3852. <https://doi.org/10.3390/su16093852>
- Pattanawanidchai, S., Sac-Oui, P., Na-Lumpang, T., Loykulnant, S., and Kuankhamnuan, T.,

- Reduction in soil compaction by utilization of waste tire rubber. *Sustainability* 15, 2023, pp. 12174. <https://doi.org/10.3390/su151612174>
8. Macuh, B., Varga, R., and Jelušič, P., Use of lignin, waste tyre rubber and waste glass for soil stabilisation. *Applied Sciences*, 14(17), 2024, pp. 7532. <https://doi.org/10.3390/app14177532>
  9. Zhang, P., Wang, C., Wu, C., Guo, Y., Li, Y., and Guo, J. A review on the properties of concrete reinforced with recycled steel fiber from waste tires. *Reviews on Advanced Materials Science*, 1(1), 2022, pp. 276–291. <https://doi.org/10.1515/rams.2022.0029>
  10. Hadiwardoyo, S. P., Andi Muhammad Ifrad, Lumingkewas, R. H., Rifai, A. I., and Wal Alif, D. I., Effect of different crumb rubber sizes on improvement of buton rock asphalt modified. *GEOMATE Journal*, 29(135), 2025, pp. 180–189. <https://doi.org/10.21660/2025.135.5198>
  11. David, J. M., De Jesus, R. M., and Mendoza Jr. R. P., Quantification of hydration products in rice husk ash (rha)-blended cement concrete with crumb waste rubber tires (cwrt) & its correlation with mechanical performance. *GEOMATE Journal*, 23(99), 2022, pp. 126–133. <https://doi.org/10.21660/2022.99.s8603>
  12. British Standards Institution. (1990). *BS 1377: Methods of test for soils for civil engineering purposes*. BSI.
  13. Ahmad, W., and Uchimura, T., The effect of moisture content at compaction and grain size distribution on the shear strength of unsaturated soils. *Sustainability*, 15(6), 2023, pp. 5123. <https://doi.org/10.3390/su15065123>
  14. Karakan, M., and Demir, Ö., The optimisation analysis of sand-clay mixtures stabilised with xanthan gum biopolymers. *Sustainability*, 13(7), 2021, pp. 3732. <https://doi.org/10.3390/su13073732>
  15. Akbarimehr D., Eslami A., and Aflaki, E., Geotechnical behaviour of clay soil mixed with rubber waste. *Journal of Cleaner Production*, 271, 2020, pp. 122632. 15. Khan, A., Radav, B. and Kumar, S., Utilization of recycled rubber crumbs and tile powder as additives to enhance clayey soil performance. *Discover Materials*, 4(1), 2024, pp. 71. <https://doi.org/10.1007/s43939-024-00146-x>
  16. Sujatha, E. R., Mahalakshmi, S. and Kannan, G., Potential of fibre reinforced and cement stabilised fibre reinforced soil blocks as sustainable building units. *Journal of Building Engineering*, 78, 2023, pp.107733. <https://doi.org/10.1016/j.jobe.2023.107733>
  17. Zafar, T., Ansari, M. A., and Husain, A., Soil stabilisation by reinforcing natural and synthetic fibers– A state of the art review. *Materials Today: Proceedings*. (2023). <https://doi.org/10.1016/j.matpr.2023.03.503>
  18. Li, H., Gao, P., Zhang, C., Guo, S., and Zhang, J., Effect of polymeric agent on the strength and water stability of cement-stabilised construction waste soil. *Sustainability*, 15(21), 2023, pp.15571. <https://doi.org/10.3390/su152115571>
  19. Sun, Z., Lu, L., Gong, J., Wei, G., and Ye, W., Shear strength performance of electrokinetic geosynthetics treated soft clay after water immersion. *Processes*, 11(2), 2023, pp. 529. <https://doi.org/10.3390/pr11020529>
  20. Han, S., Yu, D., Luo, H., Li, T., Wang, Y., and Zhang, Y., For Chapter in a Book, Experimental study on soil improvement by electrochemical injection coupled with anode movement technique. *Frontiers in Physics*, 2025, pp. 63-74. <https://doi.org/10.3389/feart.2024.1523656>
  21. Rustamajia, R. M., and Priadi, E., Stabilizing fine grained soil by electrically injecting  $\text{Ca}^{2+}$ ,  $\text{CO}_3^{2-}$ , and  $\text{HPO}_4^{2-}$  ions. *Communications in Science and Technology*, 9(1), 2024, pp. 136–143. <https://doi.org/10.21924/cst.9.1.2024.1448>
  22. Ashour, N. F., Hussein, A. K., El Sherbeeney, R. M., Omar, O. O., and Khedr, S. A., Electro-cementation of calcareous sand using colloidal silica (CS) nanoparticles and alumina powder. *Innovative Infrastructure Solutions*, 8(318), 2023, pp. 1-19. <https://doi.org/10.1007/s41062-023-01276-6>
  23. Purkis, J. M., Burrell, F., Brydie, J. R., Graham, J., Hopkinson, L., and Cundy, A. B., Electrokinetic generation of iron-rich barriers in soils: realising the potential for nuclear site management and decommissioning. *Environmental Science: Advances*, 2(4), 2023, pp. 652–662. <https://doi.org/10.1039/D2VA00308>
  24. Xie, S., Bai, Z., Shao, W., Wang, C., Qin, J., Liu, Z., and Liao, P., Phosphate removal by ex situ generated Fe hydroxides from scrap iron electrocoagulation: the critical role of coprecipitation. *Environmental Science: Advances*, 2(6), 2023, pp. 898–907. <https://doi.org/10.1039/D3VA00024A>
  25. Liao, C., Li, Q., and Lu, D., An enhanced electrokinetic/waste  $\text{Fe}(\text{OH})_3$  permeable reactive barrier system for soil remediation in sulfide mine areas. *Sustainability*, 14(22), 2022, pp. 15342. <https://doi.org/10.3390/su142215342>
  26. Furcas, F. E., Mundra, S., Lothenbach, B., and Angst, U., Speciation controls the kinetics of iron hydroxide precipitation and transformation. (preprint) *arXiv:2311.12464*, 2023. <https://doi.org/10.48550/arXiv.2311.12464>